Paweł DAWIDOWSKI[1], Jan IŻYKOWSKI[2], Przemysław BALCEREK[1]

ABB Corporate Research Centre (1), Wrocław University of Technology (2)

Fault location on double-circuit transmission line not requiring line parameters

***Abstract**. A new impedance-based algorithm for fault location on overhead double-circuit lines is presented. To assure high precision for fault location the considered calculations are based on distributed-parameter line model and the line parameters are estimated. Selected results of the evaluation of fault location accuracy with use of the signals from the ATP-EMTP simulations are presented and discussed.*

***Streszczenie.** Przedstawiono nowy impedancyjny algorytm lokalizacji zwarć w dwutorowej napowietrznej linii elektroenergetycznej. W celu zapewnienia dużej dokładności lokalizacji zastosowano model linii o parametrach rozłożonych i dokonano estymacji parametrów linii. Zamieszczono i omówiono wybrane rezultaty badań dokładności lokalizacji przeprowadzanej z użyciem sygnałów z symulacji zwarć za pomocą programu ATP-EMTP. (**Lokalizacja zwarć w dwutorowej linii przesyłowej niewymagająca znajomości parametrów linii**).*

Keywords: transmission network, double-circuit line, fault location, fault simulation.
Słowa kluczowe: sieć przesyłowa, linia dwutorowa, lokalizacja zwarć, symulacja zwarć.

Introduction

Most of power system faults occur in transmission networks, especially on overhead lines which have the highest fault rate in the system [1, 2, 3]. Under permanent faults, the line becomes switched-off by protective relays [4, 5] and the damage caused by the fault has to be repaired before the line is put back to service. The restoration can be expedited if the location of the fault is either known or can be estimated with good accuracy. For this purpose fault locators [3] are applied. Effective fault location algorithm is necessary for fast clearance of fault effects. An extra accuracy of fault location is required for very long overhead lines. Location precision for such lines is a critical factor.

Varies fault location techniques have been developed so far [3]. In particular, the methods based on travelling wave phenomenon [6–10] can assure very good fault location accuracy. Travelling waves fault location was initiated more than 60 years ago [6] and is still of great interest, which some selected references published lately [7–10] confirm evidently. However, high sampling frequency is required for such technique. Therefore, various impedance-based approaches [3] are preferred in many practical solutions and thus such the method is taken for further considerations of this paper.

First impedance-based fault locators applied three-phase voltage and current from one line end as the input signals [11, 12]. Then, unsynchronized two-end measurements [13, 14, 15] were introduced for overcoming the limitations of the one-end techniques. This was possible after developing efficient communication means for sending signals measured at remote locations. The next step was related to introducing two-end synchronized measurements, which are effectively applied for both fault location [16, 17, 18] and protection [19, 20] purposes. The satellite Global Positioning System (GPS) is commonly applied for assuring accurate synchronization of such measurements.

Recent trends of two-end fault location techniques are focused on eliminating the need for knowing line parameters what leads to getting setting-free solutions [21–24]. In this paper a new fault location algorithm which is also the setting-free is designed for a double-circuit overhead line. The authors consider overhead lines spreading over long distances, where a transposition is usually applied to assure symmetry of line phases and to minimize transmission losses. For such lines a powerful tool of symmetrical components technique is utilized. To assure the highest possible accuracy, all calculations will be based on the distributed-parameter model of an overhead line. The line parameters are estimated from available measurements and the considerations are focused on developing the algorithm which does not involve iterative calculations.

In Fig. 1 a principle of the considered fault location is depicted. The algorithm utilizes measurements of three-phase voltages and currents at both ends (S and R) of the overhead double-circuit line (LINE I and LINE II assumed as terminated at the common buses S, R):

- three-phase voltages: $\{v_S\}$, $\{v_R\}$,
- three-phase currents of faulted line circuit: $\{i_S^I\}$, $\{i_R^I\}$,
- three-phase currents of healthy line circuit: $\{i_S^{II}\}$, $\{i_R^{II}\}$.

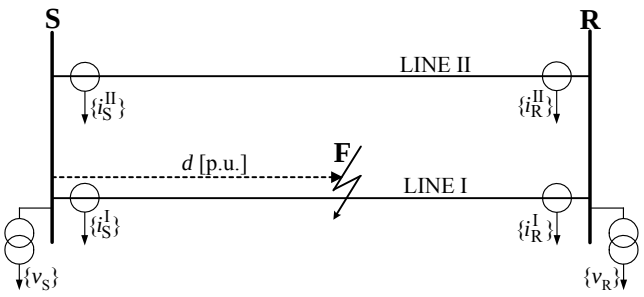

Fig. 1. Specification of two-end measurements for fault location on double-circuit line

To consider all fault types: phase-to-earth, phase-to-phase (with or without earth) and three-phase faults one can utilize the positive-sequence component as it is present in case of any fault type. Another advantage of utilizing positive-sequence is that the coupling between both line circuits is negligible and thus is out of interest.

Double-circuit overhead line fault location algorithm

Equivalent circuit-diagram of a faulted double-circuit line for the positive-sequence is presented in Fig. 2. It is assumed that the parameters of both line circuits, as having identical geometry and conductors type, are identical. The measurements from the healthy line circuit (LINE II) are utilized for determining the line parameters (identical for both circuits) and then using these parameters and the measurements of the faulted line circuit, a fault location is performed. For both purposes, i.e. for the line parameters estimation and fault location itself, the measurements from the fault interval only are utilized. An additional option for the presented fault location algorithm in which pre-fault

measurements from the faulted line circuit are utilized for the line parameters estimation also will be included.

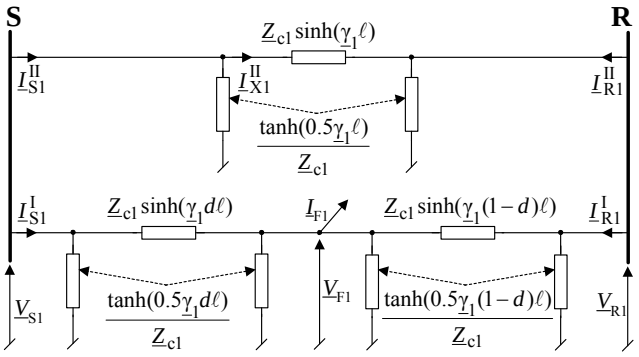

Fig. 2. Equivalent circuit diagram of faulted double-circuit line for positive-sequence

To estimate the line parameters, the following unknowns have to be taken into account: surge impedance ($\underline{Z}_{c1}$), propagation constant ($\underline{\gamma}_1$) and actual length (ℓ) of the overhead line. For fault location procedure the total length of the overhead line could be known as a sum of distances between overhead line towers. However, an actual length may differ due to a line sag and the temperature of a particular wire. Therefore, one needs to take into account the actual length of the overhead line wire. To resolve this problem it can be noticed that the propagation constant and the line length could be treated as one unknown, i.e. the product of them: ($\underline{\gamma}_1\ell$). This is so since a separation of those unknowns is not necessary for fault location calculations. If the relative distance to the fault is calculated, one can utilize the distance between all towers as a line length. Therefore, these two unknowns will be estimated together. This will limit the number of unknowns to two: the surge impedance ($\underline{Z}_{c1}$) and the propagation constant multiplied by line length ($\underline{\gamma}_1\ell$). So, two linearly independent equations are required to estimate these parameters of the overhead line [21].

For determining the auxiliary current in the healthy line circuit (Fig. 2), the voltage and current from the sending line end S (thus this auxiliary current will be marked with the superscript (S)) of this circuit can be utilized:

$$\underline{I}^{II(S)}_{X1} = \underline{I}^{II}_{S1} - \frac{\tanh(0.5\underline{\gamma}_1\ell)}{\underline{Z}_{c1}}\underline{V}_{S1} \tag{1}$$

Analogously, using the signals from the receiving line end R one gets the alternative form for the auxiliary current which is now marked with the superscript (R):

$$\underline{I}^{II(R)}_{X1} = -\underline{I}^{II}_{R1} + \frac{\tanh(0.5\underline{\gamma}_1\ell)}{\underline{Z}_{c1}}\underline{V}_{R1} \tag{2}$$

If (1) and (2) are combined, the following expression is obtained:

$$\underline{I}^{II}_{R1} + \underline{I}^{II}_{S1} = \frac{\tanh(0.5\underline{\gamma}_1 l)}{\underline{Z}_{c1}}\left(\underline{V}_{R1} + \underline{V}_{S1}\right) \tag{3}$$

Equation (3) contains the unknown line parameters. A second equation necessary to estimate these parameters can be derived if one considers the voltage loop of the healthy line circuit:

$$\underline{V}_{S1} - \underline{V}_{R1} = \underline{Z}_{c1}\sinh(\underline{\gamma}_1\ell)\underline{I}^{II(S)}_{X1} \tag{4}$$

If one substitutes (1) into (4), the following expression is obtained:

$$\underline{I}^{II}_{S1}\underline{Z}_{c1}\sinh(\underline{\gamma}_1\ell) = \underline{V}_{S1}\cosh(\underline{\gamma}_1 l) - \underline{V}_{R1} \tag{5}$$

By combining (3) and (5) and with performing appropriate rearrangements, the hyperbolic cosine of the first unknown ($\underline{\gamma}_1\ell$) can be expressed only by the measured signals of the healthy line circuit:

$$\cosh(\underline{\gamma}_1\ell) = \frac{\underline{V}_{R1}\underline{I}^{II}_{R1} - \underline{V}_{S1}\underline{I}^{II}_{S1}}{\underline{V}_{S1}\underline{I}^{II}_{R1} - \underline{V}_{R1}\underline{I}^{II}_{S1}} \tag{6}$$

In addition, utilizing (6) and the hyperbolic identity one obtains:

$$\sinh(\underline{\gamma}_1\ell) = \pm\frac{\sqrt{[(\underline{V}_{R1})^2 - (\underline{V}_{S1})^2]\cdot[(\underline{I}^{II}_{R1})^2 - (\underline{I}^{II}_{S1})^2]}}{\underline{V}_{S1}\underline{I}^{II}_{R1} - \underline{V}_{R1}\underline{I}^{II}_{S1}} \tag{7}$$

Then, by substituting (6) and (7) into (5), the surge impedance is determined in the following form:

$$\underline{Z}_{c1} = \pm\sqrt{\frac{(\underline{V}_{R1})^2 - (\underline{V}_{S1})^2}{(\underline{I}^{II}_{R1})^2 - (\underline{I}^{II}_{S1})^2}} \tag{8}$$

Both, (7) and (8) have two complex number solutions. Selection of proper solutions is obtained without difficulties. As for example, the solution which gives positive real part of $\underline{Z}_{c1}$ (8) should be selected as a proper one for the surge impedance.

The relative distance to a fault d [p.u.] is the next unknown in this analysis. It can be derived if one calculates the voltage at the fault point utilizing firstly signals from the sending line end S:

$$\underline{V}^{(S)}_{F1} = \underline{V}_{S1} - \underline{Z}_{c1}\sinh(\underline{\gamma}_1 d\ell)\cdot[\underline{I}^{I}_{S1} - \frac{1}{\underline{Z}_{c1}}\tanh(0.5\underline{\gamma}_1 d\ell)\underline{V}_{S1}] \tag{9}$$

Similar expression can be obtained by usage of signals from the receiving line end R:

$$\begin{aligned}\underline{V}^{(R)}_{F1} = {} & \underline{V}_{R1} - \underline{Z}_{c1}\sinh[\underline{\gamma}_1(1-d)\ell)\underline{I}^{I}_{R1} \\ & + \sinh[(1-d)\underline{\gamma}_1\ell)\underline{I}^{I}_{R1}\tanh(0.5(1-d)\underline{\gamma}_1\ell)\underline{V}_{R1}\end{aligned} \tag{10}$$

Comparison of (9) and (10) leads to the following formula for the sought distance to fault point F:

$$d = \frac{\tanh^{-1}\left(\dfrac{\underline{V}_{R1}\cosh(\underline{\gamma}_1\ell) - \underline{Z}_{c1}\sinh(\underline{\gamma}_1\ell)\underline{I}^{I}_{R1} - \underline{V}_{S1}}{\sinh(\underline{\gamma}_1\ell)\underline{V}_{R1} - \underline{Z}_{c1}\cosh(\underline{\gamma}_1\ell)\underline{I}^{I}_{R1} - \underline{Z}_{c1}\underline{I}^{I}_{S1}}\right)}{\underline{\gamma}_1\ell} \tag{11}$$

in which the line parameters for the positive-sequence are yet involved.

After substituting the surge impedance (8), hyperbolic sine (7) and hyperbolic cosine (6) into the derived formula for the distance to a fault (11) one obtains the relation between the distance to a fault and the voltages and currents measured at both ends of the line, in both line circuits, in the following compact form:

$$(12)\quad d = \left| \frac{\tanh^{-1}\left(\sqrt{\frac{\underline{A}_4}{\underline{A}_3}} \cdot \frac{(\underline{A}_1 \underline{V}_{R1} - \underline{A}_3 \underline{I}^{I}_{R1} - \underline{A}_2 \underline{V}_{S1})}{(\underline{A}_4 \underline{V}_{R1} - \underline{A}_1 \underline{I}^{I}_{R1} - \underline{A}_2 \underline{I}^{I}_{S1})} \right)}{\cosh^{-1}\left(\frac{\underline{A}_1}{\underline{A}_2} \right)} \right|$$

where:

$$\underline{A}_1 = \underline{V}_{R1} \underline{I}^{II}_{R1} - \underline{V}_{S1} \underline{I}^{II}_{S1},$$

$$\underline{A}_2 = \underline{V}_{S1} \underline{I}^{II}_{R1} - \underline{V}_{R1} \underline{I}^{II}_{S1},$$

$$\underline{A}_3 = \underline{V}^2_{R1} - \underline{V}^2_{S1},$$

$$\underline{A}_4 = (\underline{I}^{II}_{R1})^2 - (\underline{I}^{II}_{S1})^2,$$

or alternatively when applying the pre-fault signals ('pre' in the subscripts of the signals will be used) from the faulted line circuit to estimation of the line parameters:

$$\underline{A}_1 = \underline{V}_{R1\_pre} \underline{I}^{I}_{R1\_pre} - \underline{V}_{S1\_pre} \underline{I}^{I}_{S1\_pre},$$

$$\underline{A}_2 = \underline{V}_{S1\_pre} \underline{I}^{I}_{R1\_pre} - \underline{V}_{R1\_pre} \underline{I}^{I}_{S1\_pre},$$

$$\underline{A}_3 = (\underline{V}_{R1\_pre})^2 - (\underline{V}_{Sl\_pre})^2,$$

$$\underline{A}_4 = (\underline{I}^{I}_{R1\_pre})^2 - (\underline{I}^{I}_{S1\_pre})^2.$$

The sought distance to a fault is a real number and thus to assure obtaining this in practical calculations, an absolute value of (11) is considered in (12).

Simulation test results

To test the presented algorithm the ATP-EMTP [25, 26] model has been developed to generate the synchronized current and voltage signals. Schematic diagram of the modelled 400 kV network is presented in Fig 3.

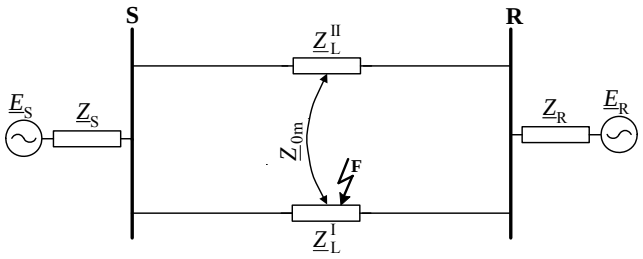

Fig. 3. Schematic diagram of modelled transmission network with double-circuit line

The 400 kV, 400 km double-circuit line of the following data for the positive-sequence, zero-sequence and mutual zero-sequence, respectively, was modelled:

- impedances:

$$Z'_{1L} = (0.0276 + \mathrm{j}0.3151)\ \Omega/\mathrm{km},$$

$$Z'_{0L} = (0.275 + \mathrm{j}1.0265)\ \Omega/\mathrm{km},$$

$$\underline{Z}'_{0m} = (0.20 + \mathrm{j}0.628)\ \Omega/\mathrm{km},$$

- shunt capacitances:

$$C'_{1L} = 13.0\ \mathrm{nF/km},$$

$$C'_{0L} = 8.5\ \mathrm{nF/km},$$

$$C'_{0m} = 5.0\ \mathrm{nF/km}.$$

The short circuit impedances for both equivalent systems ($\underline{Z}_S$, $\underline{Z}_R$) [27] at the overhead line terminals, representing the line vicinity, have been taken as 5 GVA. To force the power flow from the sending end S to the receiving one R, the equivalent voltage source at the receiving end ($\underline{E}_R$) was lagged by 15°, in relation to the voltage source at the sending end ($\underline{E}_S$).

The developed ATP-EMTP model includes voltage and current instrument transformers with errorless transformation. This was assumed in order to test an accuracy of the presented fault location accuracy alone. Anti-aliasing low-pass analogue filters with a cut-off frequency of 350 Hz were modelled in both current and voltage measurement chains. A/D conversion was performed at 1000 Hz sampling frequency and phasors of the processed signals were determined using the following pair of orthogonal filters [28, 29]:

- cosine full-cycle Fourier filter,
- cosine full-cycle Fourier filter with a delay by a quarter of the fundamental frequency cycle (by 5 samples).

The assumed filtration enables effective rejection of d.c. components in the processed signals. Final result for the distance to a fault was obtained by averaging within the 3rd period of fault interval.

Versatile simulations of faults in the test transmission network considering different fault resistance, place and fault inception angle have been simulated [21]. The selected representative results for the distance to a fault calculations are presented in Table 1. For single-phase-to-earth fault (a–E) a fault resistance was assumed as 10 Ω, while in case of inter-phase faults (a–b, a–b–E, a–b–c): 1 Ω.

Table 1. Results of fault location for different fault types

Actual distance to fault	Fault type			
	a–E	a–b	a–b–E	a–b–c
d_{actual} [p.u.]	d [p.u.]			
0.2	0.2000	0.1999	0.1998	0.2005
0.4	0.4001	0.4001	0.4001	0.4002
0.6	0.5999	0.6004	0.6003	0.5998
0.8	0.8000	0.7997	0.7998	0.7997

The determined values of the distance to a fault are very close to the actual distances, i.e. applied in the simulations. In Table 1 the fault location errors do not exceed 0.05% and it is similarly for the other cases not presented here. This is so due to applying the distributed-parameter line model and efficient digital filtration. Such accurate fault location has been achieved under assuming errorless transformation of instrument transformers. In practice, with accounting for the actual transformation errors in both voltage and current measuring channels one has to expect the resultant error higher but not exceeding 1% level, which is acceptable for practical applications. Otherwise, the instrument transformers have to be calibrated to improve fault location accuracy.

Conclusions

New fault location algorithm for a double-circuit overhead line which processes two-end synchronized measurements of voltages and currents has been presented. This is distinctive that a distributed-parameter line model is taken into account and the required calculations are non-iterative. The presented algorithm is a setting-free solution since it does not require to know line parameters.

Utilizing signals from a healthy circuit, the line parameters are estimated under an assumption that these parameters are identical for both circuits. However, use of pre-fault measurements from a faulted line circuit for the line parameters estimation has been included as the additional option.

The presented algorithm has been tested successfully with use of ATP-EMTP simulation of series of different faults on the test 400 kV, 400 km double-circuit transmission line. The achieved accuracy is very high due to applying the distributed-parameter line model and efficient digital filtration.

REFERENCES

[1] Kacejko P., Machowski J., Zwarcia w systemach elektroenergetycznych, *WNT*, Warszawa, 2002

[2] Kremens Z., Sobierajski M., Analiza systemów elektroenergetycznych, *WNT*, Warszawa, 1996

[3] Saha M.M., Iżykowski J., Rosołowski E., Fault location on power networks, *Springer*, London, 2010

[4] Winkler W., Wiszniewski A., Automatyka zabezpieczeniowa w systemach elektroenergetycznych, *WNT*, Warszawa, 1999

[5] Synal B., Rojewski W., Zabezpieczenia elektroenergetyczne: podstawy, *INPE,* Bełchatów, 2008

[6] Lewis L., Travelling wave relations applicable to power system fault locators, *AIEE Transactions*, Vol. 1951,1671–1680

[7] Glik K., Rasolomampionona D.D., Kowalik R., Detection, classification and fault location in HV lines using travelling waves, *Przegląd Elektrotechniczny (Electrical Review),* 88 (2012), nr 1a, 269–275

[8] Tabatabaei A., Mosavi M-R, Rahmati A., Fault location techniques in power system based on traveling wave using wavelet analysis and GPS timing, *Przegląd Elektrotechniczny* (*Electrical Review*), 88 (2012), nr 6, 347–350

[9] Liu Y., Sheng G., He Z., Jiang X., A traveling wave fault location method for earth faults based on mode propagation time delays of multi-measuring points, *Przegląd Elektrotechniczny* (*Electrical Review*), 88 (2012), nr 3a, 254–258

[10] Siozinys V., Markevicius L.A, The influence of corona effect on traveling wave based transmission line protection distance to fault error calculation, *Przegląd Elektrotechniczny* (*Electrical Review*), 88 (2012), nr 7b, 208–210

[11] Saha M.M., Wikstrom K., Iżykowski J., Rosołowski E., New accurate fault location algorithm for parallel lines, *Proc. of IEE Conference on Developments in Power System Protection*, Publ. Issue 479, pp. 407–410

[12] Wiszniewski A., Dokładna lokalizacja miejsca zwarcia w liniach napowietrznych elektroenergetycznych, *Przegląd Elektrotechniczny* (*Electrical Review*), 1984, nr 2, 41–44

[13] Iżykowski J., Moląg R., Rosołowski E., Saha M.M., Accurate location of faults on power transmission lines with use of two-end unsynchronized measurements. IEEE Transactions on Power Delivery, Vol. 21, No. 2, April 2006, pp. 627-633

[14] Rosołowski E., Iżykowski J., Saha M.M., Balcerek P., Fulczyk M., Accurate transmission line fault location using two-terminal data without time synchronisation, *Przegląd Elektrotechniczny* (*Electrical Review*), 2009, nr 6, 170–174

[15] Johns A.T., Jamali S., Accurate fault location technique for power transmission lines, *Proc. Inst. Elect. Eng., C*, vol. 137, nr 6, 1990, 395–402

[16] Kezunovic M., Perunicic B., Automated transmission line fault analysis using synchronized sampling at two ends, *IEEE Trans. on Power Systems*, PS–11, 1996, 441–447

[17] Wang C., Dou C.X., Li X.B., A WAMS/PMU-based fault location technique, *Electric Power Systems Research*, 2007, Vol. 77, nr 8, 936–945

[18] Iżykowski J., Rosołowski E., Synchroniczne pomiary rozproszone w zastosowaniu do lokalizacji zwarć w liniach napowietrznych, *Przegląd Elektrotechniczny* (*Electrical Review*), 2009, nr 11, 21–25

[19] Solak K., Rebizant W., Differential protection with better stabilization for external faults, *Scientific Papers of the Institute of Electrical Power Engineering of the Wrocław University of Technology: Present Problems of Power System Control*, 2011, nr 1, 39-48

[20] Łukowicz M., New method of data transmission delay estimation for feeder differential protection, *Scientific Papers of the Institute of Electrical Power Engineering of the Wrocław University of Technology: Present Problems of Power System Control*, 2011, nr 1, 97-107

[21] Dawidowski, Balcerek P., Iżykowski J., Nieiteracyjny algorytm lokalizacji zwarć w linii dwutorowej z estymacją jej parametrów, *Materiały VII Konferencji Naukowo-Technicznej: Sieci Elektroenergetyczne w Przemyśle i Energetyce*, Szklarska Poręba, 19–21.09.2012, 6 p.

[22] Apostolopoulos C.A., Korres G.N., A novel fault-location algorithm for double-circuit transmission lines without utilizing line parameters, *IEEE Transactions on Power Delivery*, vol. 26, issue 3, July 2011, 1467–1478

[23] Preston G., Radojevic Z., Kim C.H., Terzija V., New setting-free fault location algorithm based on synchronized sampling, *IET Generation, Transmission & Distribution*, 2011, vol. 5, nr 3, 376-383

[24] Liao Y., Elangovan S., Unsynchronised two-terminal transmission-line fault-location without using line parameters, *IEE Proc. – Gener., Transm. and Distribut.*, 2006, vol. 153, nr 6, 639–643

[25] Dommel H.W., Electromagnetic Transients Program, *Manual*, Bonneville Power Administration, Portland, 1986

[26] Rosołowski E., Komputerowe metody analizy elektromagnetycznych stanów przejściowych, *Oficyna Wydawnicza Politechniki Wrocławskiej*, Wrocław, 2009

[27] Sowa P., Dynamiczne układy zastępcze w analizie elektromagnetycznych stanów przejściowych. *Wydawnictwo Politechniki Śląskiej*, Gliwice, 2011

[28] Rosołowski E., Cyfrowe przetwarzanie sygnałów w automatyce elektroenergetycznej, *Wydawnictwo Exit*, Warszawa, 2002

[29] Rebizant W., Szafran J., Wiszniewski A., Digital signal processing in power system protection and control, *Springer*, London, 2011

***Authors**: dr inż. Paweł Dawidowski, ABB Corporate Research Centre, Kraków, E-mail: pawel.dawidowski@pl.abb.com; prof. dr hab. inż. Jan Iżykowski, Wrocław University of Technology, Institute of Electrical Power Engineering, ul. Wybrzeże St. Wyspiańskiego 27, 50-370 Wrocław, E-mail: jan.izykowski@pwr.wroc.pl; dr inż. Przemysław Balcerek,, ABB Corporate Research Centre, Kraków, E-mail: przemyslaw.balcerek@pl.abb.com.*